

## Strong color fields and heavy flavor production

I. Bautista and C. Pajares

*IGFAE and Departamento de Física de Partículas, Universidad de Santiago de Compostela, ES-15706 Santiago de Compostela, Spain*

(Received 8 July 2010; published 30 September 2010)

The clustering of color sources provides a natural framework for soft partonic interactions producing strong color fields. We study the consequences of these color fields in the production of heavy flavor and the behavior of the nuclear modification factor.

DOI: [10.1103/PhysRevC.82.034912](https://doi.org/10.1103/PhysRevC.82.034912)

PACS number(s): 25.75.Dw

### I. INTRODUCTION

Heavy flavor production in heavy-ion collisions is an ideal probe to study the early time dynamics of these nuclear collisions. Several theoretical studies predict [1] a substantial enhancement of open charm production associated with deconfined parton matter relative to the case of a purely hadronic scenario without quark-gluon plasma formation. Recent studies point out that the dynamics of heavy quarks is dominated by partonic interactions in a strongly coupled plasma modeled neither by hadronic interactions nor by color screening alone [2]. Therefore, these quarks are very relevant in the study of the initial state of the collision. Owing to difficulties in reconstructing the  $D$ -meson decay vertex, RHIC experiments have measured open charmed quarks indirectly, via the semileptonic decay to nonphotonic electrons or muons [3,4]. In the standard picture charm quarks are produced by initial gluon fusion and their production rates are expected to be well described by perturbative quantum chromodynamics (pQCD) at fixed order plus next-to-leading logarithms (FONLL) [5]. The suppression of single, nonphotonic electrons or muons at RHIC is usually attributed to heavy-quark energy loss. As a charmed quark of energy  $E$  cannot radiate gluons forming an angle below  $\arcsin(m/E)$  (dead cone effect), it is expected that heavy quarks lose less energy than light quarks [6], but the suppression experimentally observed is similar. In fact, many calculations based on energy loss via hard scattering [7] or via multiple soft collisions [8] obtained less suppression than the experimental data when the beauty contribution is taken into account. Similar results are obtained in evaluations based on medium interactions or collisional dissociation [9]. However, it has been argued [10,11] that under the assumption of an enhancement of the heavy-quark baryon-to-meson ratio, analogous to the case of the proton-to-pion and the  $\Lambda$ -to-kaon ratios measured in Au-Au collisions at RHIC, it is possible to achieve a larger suppression of the nuclear modification factor. This is possible because the heavy-quark mesons have a larger branching ratio to decay inclusively into electrons as compared to heavy-quark baryons and therefore, when the former are less copiously produced in a heavy-ion environment, the nuclear modified factor decreases, even in the absence of heavy-quark energy loss. Indeed the single nonphotonic nuclear modified factor,  $R_{AA}^e$ , can be expressed as [12]  $R_{AA}^e = R_{AA}^{D+\Lambda} F$ , where  $R_{AA}^{D+\Lambda}$  is the nuclear modified factor for  $D$  and  $\Lambda_c$ , that is,

$$R_{AA}^{D+\Lambda} = \frac{N_{AA}^D + N_{AA}^\Lambda}{N_{\text{coll}}(N_{pp}^D + N_{pp}^\Lambda)}, \quad (1)$$

with  $N^D$  and  $N^\Lambda$  the produced  $D$  and  $\Lambda$  in  $AA$  or  $pp$  collisions and  $N_{\text{coll}}$  the number of collisions at a given centrality. The factor  $F$  is given by the expression

$$F = \frac{(1+a)(1+xCa)}{(1+Ca)(1+xa)} \quad (2)$$

where  $a$  and  $Ca$  are the charmed baryon-to-meson ratios in proton-proton and  $AA$  collisions, respectively. Therefore  $C$  represents the enhancement factor for the ratio of charm baryons to mesons in  $AA$  as compared to  $pp$  collisions, and  $x$  is the ratio between the branching ratios for the inclusive decay of  $\Lambda$  and  $D$  into electrons:

$$a = \left(\frac{\Lambda}{D}\right)_{pp}, \quad Ca = \left(\frac{\Lambda}{D}\right)_{AA}, \quad x = \frac{B^{\Lambda \rightarrow e}}{B^{D \rightarrow e}}. \quad (3)$$

In [12]  $x$  has been estimated to be 0.14. As long as  $C$  is larger than 1 the factor  $F$  becomes less than 1 and  $R_{AA}^e < R_{AA}^{D+\Lambda}$ . The main question to solve is whether the expected charmed baryon-to-meson expected enhancement is large enough to explain the difference with the experimental data.

In a high-energy heavy-ion collision, strong color fields are expected to be produced between the partons of the projectile and target [13–15]. These color fields are similar to those that appear in the glasma [16] produced in the color glass condensate (CGC). In a string heavy-quark pairs are produced via the Schwinger mechanism with a rate  $\Gamma_{Q\bar{Q}} = \exp[-\frac{\pi m_Q^2}{k}]$ , where  $k$ , is the effective string tension, proportional to the strength of the field (for a single string  $k_1 \sim 1$  GeV/fm). Longitudinal string models predict for heavy flavor a very suppressed production rate, since

$$\frac{\Gamma_{Q\bar{Q}}}{\Gamma_{q\bar{q}}} = \exp\left[\frac{-\pi}{k_1}(m_Q^2 - m_q^2)\right] \ll 1 \quad (4)$$

for  $Q = c$  and  $q = u, d$ . The color in these strings is confined to a small area in the transverse space,  $\pi r_0^2$ , with  $r_0 \simeq 0.25$  fm. In a central heavy-ion collision many strings are formed between the partons of the projectile and target in a limited collision area, starting to overlap each other, forming clusters. The field strength of the cluster is proportional to the square root of the number of strings. So, for a cluster of nine strings, the string tension increases more than eight orders of magnitude, becoming comparable to the initial FONLL pQCD. The effect of strong color fields for open charm has been investigated before [13], showing that a three-fold increase of the effective string tension results in a sizable enhancement of the total charm cross section and the nuclear

modified factor shows a suppression at moderate  $p_T$  consistent with the RHIC data.

In this paper, we study the effects of strong color fields in the framework of percolation of strings [17]. In this framework, a strong color field is obtained inside the clusters formed by the overlapping of individual strings. The clusters behave like individual strings with a higher string tension owing to the higher color field, and their energy momentum is the sum of the energy-momenta of individual strings. The color field of the string is stretched between a quark and an antiquark or between a diquark and a quark located at the extremes of the string. In the case of a cluster, instead of quarks or antiquarks we have complexes  $Q$  and  $\bar{Q}$  formed from the different quarks and their antiquarks or diquarks and quarks at the extremes of the individual strings [18,19]. The clusters behave like strings with complexes  $Q\bar{Q}$ , located at the end, decaying into new pairs  $Q\bar{Q}$ ,  $\bar{Q}Q$ , until they come to objects with mass comparable to hadron masses, which are identified with the known hadrons by combining the produced quarks or antiquarks with the appropriate statistical weights. In this way, the production of baryons and antibaryons is enhanced with the number of strings in the cluster. The cluster not only has a stronger color field than the individual string giving rise to a mass-enhancement effect but also enhances the production of baryons relative to mesons owing to the increasing probability of getting three quarks or three antiquarks from the complex  $Q\bar{Q}$  [18]. This second effect is similar to what happens in coalescence or recombination models [20,21].

The percolation of strings incorporates to some extent the recombination of flavors in a dynamical way. Indeed a dynamical quark recombination model has shown a sizable suppression factor for the nonphotonic electron nuclear modification factor [12].

We evaluate the nuclear modification factor for  $D_0$ ,  $\Lambda_c$ , and  $B$  at RHIC energies, computing also the baryon-to-meson ratio in  $AA$  and  $pp$  collisions. We observe also in  $pp$  a moderate enhancement of the ratio as a function of the transverse momentum, which has consequences concerning the value of  $F$  and therefore the rate of the nonphotonic electron suppression. The plan of the paper is as follows: In the next section, we introduce briefly the percolation of the strings, and then we present our results and conclusions.

## II. THE STRING PERCOLATION MODEL

In the string percolation model [17,22–25], multiparticle production is described in terms of color strings stretched between the partons of the projectile and the target. With increasing energy and/or atomic number of the colliding particles, the number of strings,  $N_s$ , grows and they start to overlap forming clusters, very much like disks in two-dimensional percolation theory. At a certain critical density, a macroscopical cluster appears, which marks the percolation phase transition. This density corresponds to the value  $\eta_c = 1.2$ – $1.5$  (depending on the profile function of the colliding nuclei), where  $\eta = N_s S_1 / S_A$  and  $S_A$  stands for the overlapping area of the colliding objects. A cluster of  $n$  strings behaves like a single string with energy-momentum corresponding

to the sum of individual ones and with a higher color field corresponding to the vectorial sum in color space of the color fields of the individual strings. In this way, the mean multiplicity  $\langle \mu_n \rangle$  and the mean transverse momentum squared  $\langle p_{Tn}^2 \rangle$  of the particles produced by a cluster are given by

$$\langle \mu_n \rangle = \sqrt{\frac{n S_n}{S_1}} \langle \mu_1 \rangle \quad \text{and} \quad \langle p_{Tn}^2 \rangle = \sqrt{\frac{n S_1}{S_n}} \langle p_{T1}^2 \rangle, \quad (5)$$

where  $\langle \mu_1 \rangle$  and  $\langle p_{T1} \rangle$  are the corresponding quantities in a single string.

In the limit of high density of strings, Eqs. (5) transform into [24]

$$\langle \mu \rangle = N_s F(\eta) \langle \mu_1 \rangle \quad \text{and} \quad \langle p_T^2 \rangle = \frac{\langle p_{T1}^2 \rangle}{F(\eta)} \quad (6)$$

with  $F(\eta) = \sqrt{\frac{1-e^{-\eta}}{\eta}}$ .

For a specific kind of particle  $i$ , we will use  $\langle \mu_1 \rangle_i$ ,  $\langle p_{T1}^2 \rangle_i$ ,  $\langle \mu_n \rangle_i$ , and  $\langle p_{Tn}^2 \rangle_i$  for the corresponding quantities. To compute the multiplicities, we must know  $N_s$  and  $\mu_1$  (so for a fixed centrality, knowing  $N_s$  we deduce the density  $\eta$ ). Up to RHIC energies, in the central rapidity region  $N_s$  is approximately twice the number of collisions,  $N_{\text{coll}}$ . However,  $N_s$  is larger than  $2N_{\text{coll}}$  at RHIC and LHC energies, in the same way as in nucleon-nucleon collisions. According to color exchange models, such as the dual parton model or the quark gluon string model [26,27], the number of produced strings,  $N_s$ , is larger than two, starting at RHIC energies. Indeed, at high enough energy the strings are stretched not only between the diquarks (quarks) and quarks (diquarks) of the projectile and target, respectively, but also between quarks (antiquarks) and antiquarks (quarks) of the sea. As the energy increases, more  $q\bar{q}$  or  $qq\bar{q}\bar{q}$  are formed and  $N_s$  becomes larger than two. For the same reason in  $AA$  collisions,  $N_s$  at high energy is larger than  $2N_{\text{coll}}$ . In this work we take the values of  $N_s$  from a Monte Carlo calculation based on the quark-gluon string model [28].

Concerning the transverse momentum distribution, one needs the distribution  $g(x, p_T)$  for each cluster and the mean square transverse momentum distribution of the clusters  $W(x)$ , where  $x$  is the inverse of the mean of the squared transverse momentum of each cluster, which is related to the cluster size by Eq. (5). We take  $g(x, p_T^2) = \exp(-p_T^2 x)$  as it is used for fragmentation of the Lund string. For the weight function  $W(x)$  we take the gamma distribution. The generalized gamma distributions are unique distributions stable under the cluster-size transformations [22,29,30]; for simplicity we choose gamma distribution [22]:

$$W(x) = \frac{\gamma(\gamma x)^{k-1}}{\Gamma(k)} \exp(-kx) \quad (7)$$

with

$$\gamma = k/\langle x \rangle \quad (8)$$

and

$$\frac{1}{k} = \frac{\langle x^2 \rangle - \langle x \rangle^2}{\langle x \rangle^2}. \quad (9)$$

The function  $k$  measures the width of the distribution (7) and is the inverse of the normalized dispersion of the transverse momentum squared. The function  $k$  depends on the density of strings,  $\eta$ .

The transverse momentum distribution  $f(p_T, y)$  of particle  $i$  is

$$\begin{aligned} f(p_T, y) &= \frac{dN}{dp_T^2 dy} = \int_0^\infty dx W(x) g(p_T, x) \\ &= \frac{dN}{dy} \frac{k-1}{k} F(\eta) \frac{1}{[1 + F(\eta) p_T^2 / k \langle p_T^2 \rangle_{1i}]^k}. \end{aligned} \quad (10)$$

The formula (10) is valid for all types of collisions, all energies, and also all kind of flavors. Later we will extend (10) for baryons. The function  $k(\eta)$  was determined by comparing (10) to RHIC data. The function  $k$  decreases with  $\eta$  up to values  $\eta \simeq 1$  (peripheral Au-Au collisions at RHIC energies) and from there it increases slowly. This behavior was expected. In fact, at low density there is no overlapping of strings and there are isolated strings; therefore  $k \rightarrow \infty$ . When the density and therefore the numerator of Eq. (9) increases then  $k$  decreases. The minimum of  $k$  will be reached where the fluctuations in the cluster size reach its maximum. Above this point, increasing  $\eta$  decreases these fluctuations and increases  $k$ . The agreement with data for  $p_T$  up to 5 GeV/c is very good [22,23].

In percolation of strings the fragmentation of a cluster of many strings is via the Schwinger mechanism, producing successive pairs  $Q\bar{Q}$ , where  $Q$  represents the complexes of quarks, diquarks, and antiquarks at the extremes of the original string. It is clear that formula (10) only contains the effect of the stronger color field of the cluster, which enhances heavy-particle production, irrespective of their being mesons or baryons, but it does not contain the breaking via flavor complexes  $Q\bar{Q}$  and therefore cannot describe baryons correctly. In previous papers [18,19,28] Monte Carlo codes were presented where this mechanism was built up, but with the approximation of fusion of only two strings [17,18] or using an effective color field [28]. To keep a closed analytical formula, incorporating the antibaryon and baryon enhancement from the mechanism depicted here, we observe that this enhancement is similar to using the formula (10) with a larger density, or equivalently with a larger  $N_s$ . This means that for antibaryons or baryons if we want to continue with formula (10) we must replace  $\eta$  by  $\bar{\eta}_B$ ,

$$\bar{\eta}_B = N_s^\alpha \eta, \quad (11)$$

and instead of the first equation (6) we must use

$$\mu_{\bar{B}} = N_s^{1+\alpha} F(\eta_B) \mu_{1\bar{B}}, \quad (12)$$

where the parameter  $\alpha$  is obtained from a fit to the experimental dependence of the  $p_T$ -integrated  $\bar{p}$  spectra with centrality [31]. The obtained value is  $\alpha = 0.09$ . In the same sense we can say that the antibaryons (baryons) probe a higher density than mesons for a fixed energy and type of collision.

Equations (10), (11), and (12) allow us to compute the antibaryon (baryon) spectra. Equations (11) and (12) replace the recombination process described in this section and it should be considered as an approximation to keep the analytical formula (10). The formulas (10), (11), and (12) are

valid for all kind of particles and not only for heavy flavor. We will show some results concerning light flavor.

### III. RESULTS

Equation (10) is limited to low and moderate  $p_T$  not higher than 4–5 GeV/c. In fact, we consider a Gaussian  $p_T$  distribution for the particles produced from the fragmentation of a string, without any power-like tail. This excludes the high- $p_T$  behavior, although our formula (10) allows for an interpolation from low to high  $p_T$ . By continuity, the high- $p_T$  suppression observed at RHIC should give rise to a suppression at moderate  $p_T$ , say 4–5 GeV/c, which is the limit where our equations apply.

To know the  $p_T$  distributions given by formula (6) we need the values of  $\langle p_T^2 \rangle_{1D} \simeq \langle p_T^2 \rangle_{1D}^2$  and  $\langle p_T^2 \rangle_{1\Lambda_c} \simeq \langle p_T^2 \rangle_{1\Lambda_c}^2$ , that is, the mean  $p_T$  of  $D$  and  $\Lambda_c$  particles produced from one string. We use  $\langle p_T \rangle_{1D} = 1.5$  GeV/c and  $\langle p_T \rangle_{1\Lambda_c} = 1.9$  GeV/c. The difference between these two values is close to the difference between the masses of  $D_0$  and  $\Lambda_c$  and also agrees with the difference between the values commonly used of primordial transverse momentum of pions and protons,  $\langle p_T \rangle_{1\pi} = 0.2$ – $0.3$  GeV/c and  $\langle p_T \rangle_{1p} = 0.6$ – $0.7$  GeV/c. For  $B$  we use  $\langle p_T \rangle_{1B} = 4.25$  GeV/c.

In formula (10) the normalization is established by the values of  $\frac{dN}{dy}$  at  $p_T = 0$ , which are computed using the formulas (6) for  $D$  and (9) for  $\Lambda_c$ . To do this, we use the values  $\mu_{1D} = \exp[-F(\eta) \frac{m_D^2}{\langle p_T \rangle_{1D}^2}] \mu_{1\pi}$  and  $\mu_{1\Lambda_c} = \exp[-F(\eta_{\Lambda_c}) \frac{m_{\Lambda_c}^2}{\langle p_T \rangle_{1\Lambda_c}^2}] \mu_{1\pi}$ , with  $\mu_{1\pi} = 0.8$  [25]. We use these functions for  $\mu_{1D}$  and  $\mu_{1\Lambda_c}$  because, for heavy particles,  $m_T^2$  is very different from  $p_T^2$ . Concerning the function  $k(\eta)$ , we take the shape and values from the studies done in Ref. [25] for AA collisions. In the case of  $pp$  collisions we take  $k(\eta) = 3.97$  at  $\sqrt{s} = 200$  GeV and  $k(\eta) = 4.07$  at  $\sqrt{s} = 5.5$  TeV. We discuss later the sensitivity of the obtained result for the ratio  $(\Lambda_c/D^0)$  to different  $k$  values.

In Fig. 1 we present our results for the nuclear modified factor  $R_{AA}$  for Au-Au collisions at RHIC for  $D^0$  (green),  $\Lambda_c$  (blue),  $B$  (orange), and  $R_{AA}^c$  using formulas (1) as a function

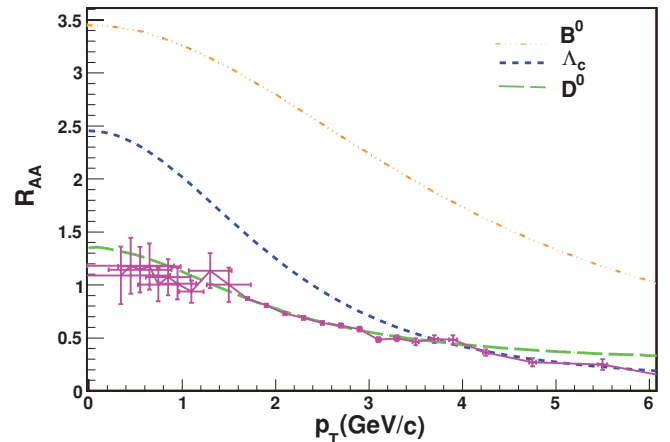


FIG. 1. (Color online)  $R_{AA}$  for Au + Au central collisions, bars is data taken from PHENIX [31].

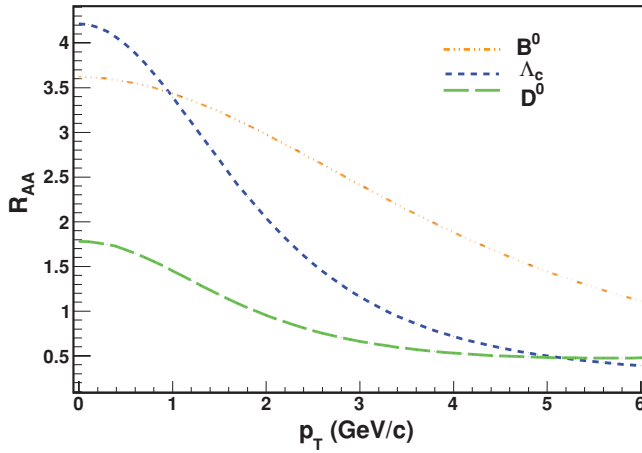


FIG. 2. (Color online)  $R_{AA}$  for Pb + Pb central collisions at  $\sqrt{s} = 5.5$  TeV.

of  $p_T^2$  compared with the experimental data on nonphotonic electrons.

The overall normalization is given by the value of  $R_{AA}$  at  $p_T^2 = 0$ , which has to do with the factor  $\exp[F(\eta_{pp}) - F(\eta_{AA})] \frac{m_D^2}{\langle p_T^2 \rangle_{1D}}$ . Since we know the number of strings produced in  $pp$  and  $AA$  collisions, we know  $\eta_{pp}$ ,  $\eta_{AA}$ ,  $F(\eta_{AA})$ , and  $F(\eta_{pp})$  and the only free parameter is  $\langle p_T^2 \rangle_{1D}$ . From the data we obtain  $\langle p_T \rangle_{1D} \sim 1.5$  GeV/c. The experimental errors allow us a 15% freedom in the value of  $\langle p_T \rangle_{1D}$ ; however, a higher value than 1.5 GeV/c would not be realistic and a lower value will give rise to a higher normalization and therefore  $R_{AA}$  for  $p_T > 4$  GeV/c will exceed the experimental data even more than with the used value. The value of  $R_{AA}$  for  $D^0$  at low  $p_T$  agrees with the results in [14,32]; for  $p_T > 4$  GeV/c we obtain an  $R_{AA}$  larger than the nonphotonic leptonic data. In Fig. 2, we present our results on  $R_{AA}$  at  $\sqrt{s} = 5.5$  TeV for a  $D^0$ ,  $\Lambda_c$ , and  $B$ . We see that, as expected, as energy increases the low- $p_T$   $R_{AA}$  increases, although the suppression at intermediate  $p_T$  is similar.

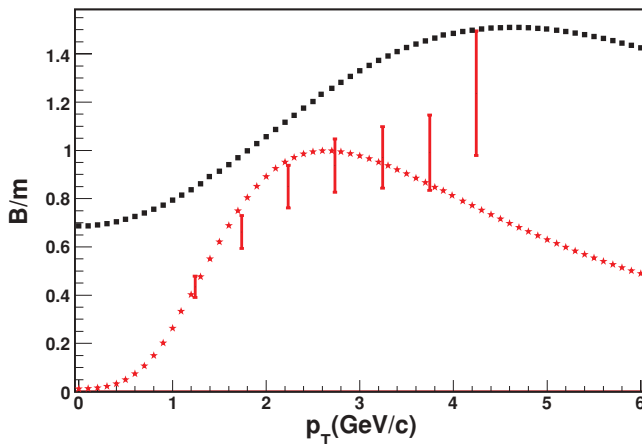


FIG. 3. (Color online) Squares are used for  $\Lambda_c/D^0$  ratio, stars are used for  $\bar{p}/\pi$  ratio, and error bars corresponds to data from PHENIX for Au-Au central collisions at  $\sqrt{s} = 200$  (GeV).

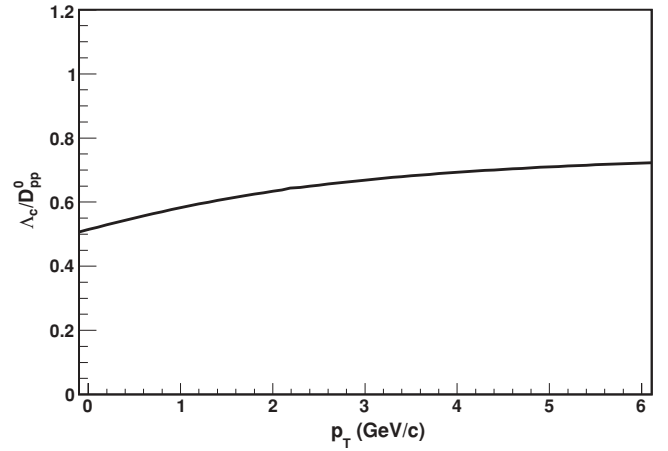


FIG. 4. Ratio  $\Lambda_c/D^0$  for  $pp$  collisions at  $\sqrt{s} = 200$  GeV.

In Fig. 3, we present the ratio  $\Lambda_c/D^0$  for Au-Au collisions at  $\sqrt{s} = 200$  GeV. We observe that the ratio increases up to a maximum of 1.45 around  $p_T \sim 4-5$  GeV/c. A very similar enhancement has been obtained in the dynamical recombination model [12].

For comparison we include also our results for  $\bar{p}/\pi$  at central Au-Au collisions together with experimental data [33]. In Fig. 4 we show the ratio  $\Lambda_c/D^0$  for  $pp$  at  $\sqrt{s} = 200$  GeV. We observe a very smooth enhancement.

In Figs. 5 and 6 we show our results for the ratio  $\Lambda_c/D^0$  at  $\sqrt{s} = 5.5$  TeV for Pb-Pb collisions and  $pp$  collisions, respectively. We observe in both of them larger enhancement than at RHIC energies, particularly in the nuclear case.

In Fig. 7 we plot the factor  $F$  at  $\sqrt{s} = 200$  GeV (blue line) and at  $\sqrt{s} = 5.5$  TeV (red line). We observe that at RHIC energies the factor  $F$  is only slightly below one, and for  $p_T \simeq 4-5$  GeV/c it is clearly over 0.5, which means that the  $\Lambda_c/D^0$  enhancement in  $AA$  collisions is not able to explain all the difference between experimentally observed suppression of  $R_{AA}$  for nonphotonic electrons and the pQCD expectations. We have studied the effects of the uncertainties in the  $k$  values for  $pp$  collisions at this energy. For reasonable alternative  $k$

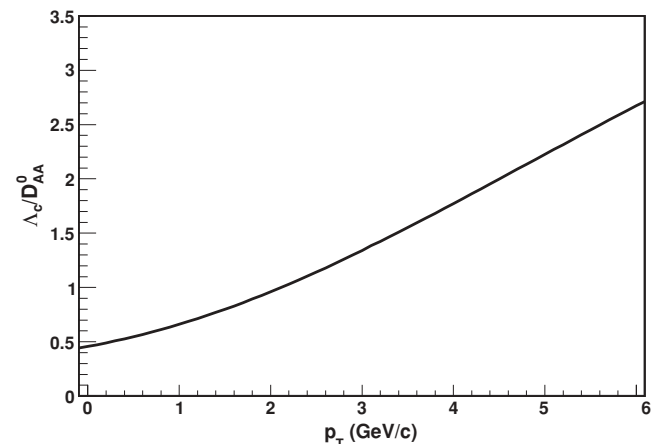


FIG. 5. Ratio  $\Lambda_c/D^0$  for Pb-Pb central collisions at  $\sqrt{s} = 5.5$  TeV.

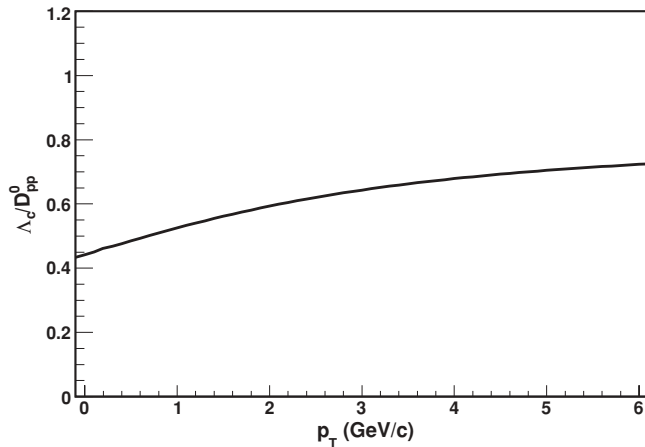


FIG. 6.  $R_{AA} \Lambda_c/D^0$  for  $pp$  collisions at  $\sqrt{s} = 5.5$  TeV.

values the enhancement of  $\Lambda_c/D^0$  in  $pp$  collisions with  $p_T$  is larger, giving rise to a lower  $C$  factor in Eq. (3) and therefore the factor  $F$  is near one, consistent with our main conclusion, namely, that the  $\Lambda_c/D^0$  enhancement is not able to explain all the difference between the experimentally observed values and the perturbative expectations.

#### IV. CONCLUSION

The overlapping of the strings formed in the collision of heavy-nuclei particles produces strong color fields that give rise to an enhancement of heavy flavor. We have computed the nuclear modification factor of  $D^0$ ,  $\Lambda_c$ , and  $B^0$  at RHIC and LHC energies for  $AA$  collisions. Referring to  $D^0$ , we obtain a good agreement at low  $p_T$  with the experimental data for the nuclear modification factor of nonphotonic electrons. For  $p_T$  values between 2 and 6 GeV/ $c$  our results obtained are over the experimental data as in pQCD.

The ratio  $\Lambda_c/D^0$  as a function of  $p_T$  for Au-Au collisions at  $\sqrt{s} = 200$  GeV is enhanced, showing a maximum around

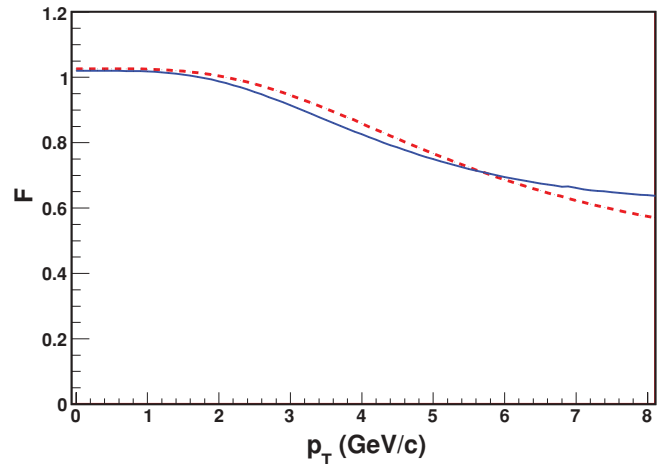


FIG. 7. (Color online) Factor  $F$  for central collisions at RHIC energies in full line and LHC energies in dashed lines.

5 GeV/ $c$ . Such an enhancement is much larger at LHC energies. However, the enhancement  $\Lambda_c/D^0$  can explain only half of the factor 2 difference between the experimental data and the pQCD expectations at RHIC energies.

In  $pp$  collisions the ratio  $\Lambda_c/D^0$  also rises as a function of  $p_T$  but very smoothly at RHIC energies. At LHC this increase is a factor of 2 between  $p_T = 0$  and  $p_T = 6$  GeV/ $c$ . The enhancements of  $\Lambda_c/D^0$  in  $AA$  and  $pp$  collisions are larger at LHC than at RHIC as was expected owing to the stronger color fields produced.

#### ACKNOWLEDGMENTS

We thank N. Armesto and A. Ayala and M. A. Braun for discussions. This research was supported by MICINN of Spain, under Grant No. FPA2008-01177, and by Xunta de Galicia.

- 
- [1] B. Muller and X. N. Wang, *Phys. Rev. Lett.* **68**, 2437 (1992); E. V. Shuryak, *ibid.* **68**, 3270 (1992).
- [2] O. Linnyk, E. L. Bratkovskaya, and W. Cassing, *Int. J. Mod. Phys. E* **17**, 1367 (2008).
- [3] J. Adams *et al.* (STAR Collaboration), *Phys. Rev. Lett.* **94**, 062301 (2005); B. I. Abelev *et al.* (STAR Collaboration), *ibid.* **98**, 192301 (2007).
- [4] S. S. Adler *et al.* (PHENIX Collaboration), *Phys. Rev. Lett.* **94**, 082301 (2005); A. Adare *et al.* (PHENIX Collaboration), *ibid.* **98**, 172301 (2007).
- [5] M. Cacciari, M. Greco, and P. Nason, *J. High Energy Phys.* **05** (1998) 007.
- [6] Y. L. Dokshitzer and D. E. Kharzeev, *Phys. Lett. B* **519**, 199 (2001).
- [7] M. Djordjevic, M. Gyulassy, R. Vogt, and S. Wicks, *Phys. Lett. B* **632**, 81 (2006).
- [8] N. Armesto, M. Cacciari, A. Dainese, C. A. Salgado, and U. A. Wiedemann, *Phys. Lett. B* **637**, 362 (2006).
- [9] A. Adil and I. Vitev, *Phys. Lett. B* **649**, 139 (2007).
- [10] G. Martinez-Garcia, S. Gadrat, and P. Crochet, *Phys. Lett. B* **663**, 55 (2008); *J. Phys. G* **35**, 044023 (2008).
- [11] D. C. Zhou, Z. Conesa del Valle, A. Dainese, H. T. Ding, and G. Martinez Garcia, *J. Phys. G* **36**, 064055 (2009).
- [12] A. Ayala, J. Magnin, L. M. Montano, and G. Toledo Sanchez, *Phys. Rev. C* **80**, 064905 (2009).
- [13] V. Topor Pop, M. Gyulassy, J. Barrette, C. Gale, S. Jeon, and R. Bellwied, *Phys. Rev. C* **75**, 014904 (2007).
- [14] V. Topor Pop, J. Barrette, and M. Gyulassy, *Phys. Rev. Lett.* **102**, 232302 (2009).
- [15] N. Armesto, M. A. Braun, E. G. Ferreira, and C. Pajares, *Phys. Lett. B* **344**, 301 (1995); J. Dias de Deus, E. G. Ferreira, C. Pajares, and R. Ugoccioni, *ibid.* **581**, 156 (2004).
- [16] D. Kharzeev and K. Tuchin, *Nucl. Phys. A* **735**, 248 (2004); L. McLerran, *J. Phys. G* **35**, 104001 (2008).
- [17] N. Armesto, M. A. Braun, E. G. Ferreira, and C. Pajares, *Phys. Rev. Lett.* **77**, 3736 (1996).
- [18] N. S. Amelin, M. A. Braun, and C. Pajares, *Z. Phys. C* **63**, 507 (1994); *Phys. Lett. B* **306**, 312 (1993).

- [19] N. S. Amelin, H. Stocker, W. Greiner, N. Armesto, M. A. Braun, and C. Pajares, *Phys. Rev. C* **52**, 362 (1995).
- [20] R. C. Hwa and C. B. Yang, *Phys. Rev. C* **65**, 034905 (2002); **67**, 059902(E) (2003).
- [21] R. J. Fries, B. Muller, C. Nonaka, and S. A. Bass, *Phys. Rev. Lett.* **90**, 202303 (2003).
- [22] J. Dias de Deus, E. G. Ferreira, C. Pajares, and R. Ugoccioni, *Eur. Phys. J. C* **40**, 229 (2005).
- [23] C. Pajares, *Eur. Phys. J. C* **43**, 9 (2005).
- [24] M. A. Braun and C. Pajares, *Phys. Rev. Lett.* **85**, 4864 (2000); *Eur. Phys. J. C* **16**, 349 (2000).
- [25] L. Cunqueiro, J. Dias de Deus, E. G. Ferreira, and C. Pajares, *Eur. Phys. J. C* **53**, 585 (2008).
- [26] A. Capella, U. Sukhatme, C. I. Tan, and J. Tran Thanh Van, *Phys. Lett. B* **81**, 68 (1979); *Phys. Rep.* **236**, 225 (1994); A. Capella, C. Pajares, and A. V. Ramallo, *Nucl. Phys. B* **241**, 75 (1984).
- [27] A. B. Kaidalov and K. A. Ter-Martirosian, *Phys. Lett. B* **117**, 247 (1982).
- [28] N. S. Amelin, N. Armesto, C. Pajares, and D. Sousa, *Eur. Phys. J. C* **22**, 149 (2001); N. Armesto, C. Pajares, and D. Sousa, *Phys. Lett. B* **527**, 92 (2002).
- [29] G. Jona-Lasinio, *Nuovo Cimento B* **26**, 99 (1975).
- [30] J. Dias de Deus, C. Pajares, and C. A. Salgado, *Phys. Lett. B* **407**, 335 (1997); A. Capella, J. Tran Thanh Van, R. Blankenbecler, C. Pajares, and A. V. Ramallo, *ibid.* **107**, 106 (1981).
- [31] PHENIX Collaboration, *Phys. Rev. Lett.* **88**, 192303 (2002).
- [32] M. G. Ryskin, A. G. Shuvaev, and Yu. M. Shabelski, *Phys. At. Nucl.* **64**, 120 (2001) [*Yad. Fiz.* **64**, 123 (2001)]; C. Merino, C. Pajares, M. M. Ryzhinskiy, Yu. M. Shabelski, and A. G. Shuvaev, [arXiv:0910.2364](https://arxiv.org/abs/0910.2364) [hep-ph].
- [33] S. S. Adler *et al.* (PHENIX Collaboration), *Phys. Rev. C* **69**, 034909 (2004).